Transition features in transonic flow around a NACA0012 airfoil by Navier-Stokes and low-order modelling

R. Bourguet[1] M. Braza[1] A. Dervieux[2] A. Sévrain[1]

[1]Institut de Mécanique des Fluides de Toulouse, France

[2]Institut National de Recherche en Informatique et en Automatique, Sophia-Antipolis, France

West-East High Speed Flow Field Conference

19-22, November 2007

Moscow, Russia

Introduction

Prediction of unsteady compressible wall flows at high Reynolds number in complex geometries in the context of multidisciplinary iterative processes :

- Multi-physic coupling : fluid/structure interaction,...
- Feedback control
- Optimal shape design

Mean : *local but faithfull approximation* of the complex physical model
$\longrightarrow$ numerical complexity reduction

In the present study : **Galerkin projection** of the compressible Navier-Stokes system onto a basis issued from a **Proper Orthogonal Decomposition** of the state variables

Physical context

- Compressible Navier-Stokes system
  - Direct simulation
  - Statistical approach - URANS
  - Spatial filtering - LES
- 2D/3D
- Unsteady simulation - instability mode capture
- Moving/deforming mesh

Physical context

- Compressible Navier-Stokes system
  - Direct simulation
  - Statistical approach - URANS
  - Spatial filtering - LES
- 2D/3D
- Unsteady simulation - instability mode capture
- Moving/deforming mesh

In the present study

- 2D compressible Navier-Stokes governing equations
- Laminar/transitional flow past an airfoil $\rightarrow$ instabilities and unsteady phenomena induced by compressibility effects
- High transonic regime

Outline

1. High transonic flow physics
   - Transitional flows in transonic regimes
   - Navier-Stokes simulation - “high-fidelity” model
2. POD-Galerkin reduced-order model
   - Optimal basis extraction by POD
   - Low-dimensional modelling
   - Validation for short time integrations
   - Stabilisation procedures
   - Low-order model robustness with respect to Reynolds number variation
   - Investigation of buffet phenomenon
3. Conclusions

Transitional flows in transonic regimes

Flow past a NACA0012 airfoil at zero angle of attack : unsteady in transonic regimes at moderate Reynolds numbers ($0.5 - 1 \times 10^4$, Bouhadji-Braza COMP&FLUIDS2003)

- from Mach number > 0.3 : oscillations in the wake
- from Mach number 0.5 to 0.7 : von Kármán instability, mode I
- from Mach number 0.75 : secondary phenomenon of lower frequency, mode II (buffet)
- at Mach number 0.85 : mode II has disappeared and mode I remains until approximately Mach number 0.95

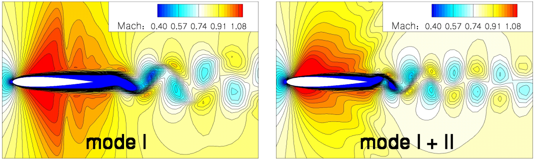

$R_e = 5000$ and $M = 0.85$: Mode I (left). $R_e = 10000$ and $M = 0.8$: Mode I and Mode II (right)

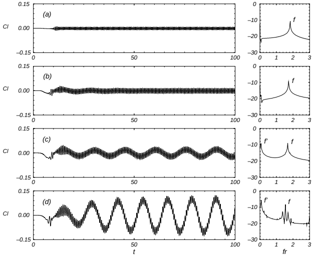

Lift coefficient : $R_e = 10000$, (a) $M = 0.5$, (b) $M = 0.7$, (c) $M = 0.75$, (d) $M = 0.8$

The "high-order" physical model

- 2D compressible Navier-Stokes system (conservative variables) :

$$U_{,t} + F_{\alpha,\alpha} = F^{\text{vis}}_{\alpha,\alpha}$$

with

$$U = \begin{bmatrix} \rho \\ \rho u_1 \\ \rho u_2 \\ \rho e \end{bmatrix}, \; F_i = \begin{bmatrix} \rho u_i \\ \rho u_i u_1 + p\delta_{1i} \\ \rho u_i u_2 + p\delta_{2i} \\ \rho u_i e + p u_i \end{bmatrix}, \; F^{\text{vis}}_i = \begin{bmatrix} 0 \\ \tau_{1i} \\ \tau_{2i} \\ \tau_{i\alpha} u_\alpha - q_i \end{bmatrix},$$

- Steady boundary conditions : no-slip on the airfoil, Dirichlet inlet, Neumann outlet (farfield : 10 $\times$ chordlengths)
- Finite volume solver : *ICARE/IMFT compressible* :
  - Convective term : second order Roe scheme
  - Diffusive term : second order central scheme
  - Time integration : fourth order Runge-Kutta scheme
  - C type mesh ($N_x = 369 \times 89$) validated for the present configurations (Bouhadji-Braza COMP&FLUIDS2003)

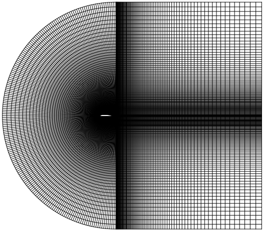

Proper Orthogonal Decomposition

Snapshots method (Sirovitch,1987)

$u^k, k = 1, N$ from N time steps $\Rightarrow U_{ij} = \frac{1}{N}(u^i, u^j) \ \Rightarrow \ \mathbf{Uc} = \lambda \mathbf{c}$

$$\text{Modes : } \Phi = \sum_{k=1}^{k=N} c_k \mathbf{u} \quad + \text{orthonormalisation.}$$

Galerkin approximation for :

$$\mathbf{u}_{,t} = \mathbf{F}(\mathbf{u}), \quad \mathbf{u} = \mathbf{u}(\mathbf{x}, t), \quad t \geq 0, \quad \mathbf{x} \in \Omega$$

$$\text{Find } \mathbf{u}(x,t) = \sum_{k=1}^{k=N_{\text{pod}}} y_k(t)\Phi_k \text{ solution of } \sum_{j=1}^{j=N_{\text{pod}}} y_{j,t}(\Phi_j, \Phi_k) = y_{k,t} \ = \ (\mathbf{Fu}, \Phi_k)$$

- POD applied to state variable fluctuations $\longrightarrow$ homogeneous boundary conditions.
- Inner product $(.,.)$ to be specified.

Proper Orthogonal Decomposition

$L^2(\Omega)^d$ inner product definition in case of vectorial quantities ($d > 1$)

- Classical choice (cf. incompressible case) : global dynamics but inconsistency

$$(s_1, s_2) = \sum_{i=1}^{4} \int_\Omega v_1^i v_2^i dx \rightarrow v^i(x,t) \approx \sum_{j=1}^{N_{\text{pod}}} y_j(t)\Phi_j^i(x) \qquad (4 \times N_x \rightarrow N_{\text{pod}})$$

- Proper dynamic for each variable : consistency but higher cost

$$\left(v_1^i, v_2^i\right) = \int_\Omega v_1^i v_2^i dx \rightarrow v^i(x,t) \approx \sum_{j=1}^{N_{\text{pod}}} y_j^i(t)\Phi_j^i(x) \qquad (4 \times N_x \rightarrow 4 \times N_{\text{pod}})$$

- Consistent inner products : global non-dimensional dynamics

$$(s_1, s_2) = \sum_{i=1}^{4} \int_\Omega \frac{v_1^i v_2^i}{\sigma_i^2} dx \rightarrow v^i(x,t) \approx \sum_{j=1}^{N_{\text{pod}}} y_j(t)\Phi_j^i(x) \qquad (4 \times N_x \rightarrow N_{\text{pod}})$$

Proper Orthogonal Decomposition

$L^2(\Omega)^d$ inner product definition in case of vectorial quantities ($d > 1$)

- Consistent inner products : global non-dimensional dynamics ($4 \times N_x \longrightarrow N_{\text{pod}}$)

$$(s_1, s_2) = \sum_{i=1}^{4} \int_\Omega \frac{v_1^i v_2^i}{\sigma_i^2} dx \quad \text{where} \quad \sigma_i^2 \text{ is } v^i \text{ time statistical variance}$$

  - Local definition :

$$\sigma_i^2(x) = \frac{1}{T} \int_{t_0}^{t_0+T} \left(v^i(x,t) - \overline{v^i(x)} \right)^2 dt \;\longrightarrow\; (s_1, s_2) = \sum_{i=1}^{4} \int_\Omega \frac{v_1^i v_2^i}{\sigma_i^2(x) + \varepsilon} dx$$

  - Global definition :

$$\sigma_i^2 = \frac{1}{T} \int_\Omega \int_{t_0}^{t_0+T} \left(v^i(x,t) - \overline{v^i(x)} \right)^2 dtdx \; > \; 0 \quad \text{no indeterminacy}$$

Navier-Stokes projection onto POD basis

- Quadratic fluxes owing to variable change (Vigo, INRIA RR, 2000)

$$U = \begin{bmatrix} \rho \\ \rho u_1 \\ \rho u_2 \\ \rho e \end{bmatrix} \to \hat{U} = \begin{bmatrix} 1/\rho \\ u_1 \\ u_2 \\ p \end{bmatrix} \to \hat{U}_{,t} + \hat{A}_\alpha \hat{U}_{,\alpha} = \hat{F}^{vis}_{\alpha,\alpha} - \hat{G}^{vis}_\alpha$$

- POD expansion and Galerkin projection, for $i = 1, \ldots, N_{POD}$

$$\left(\hat{U}_{,t} + \hat{A}_\alpha \hat{U}_{,\alpha}, \Phi_i\right) = \left(\hat{F}^{vis}_{\alpha,\alpha} - \hat{G}^{vis}_\alpha, \Phi_i\right)$$

lead to

$$\begin{cases} \dot{y}_i = C_i + \sum_{j=1}^{N_{\text{pod}}} L_{ij} y_j + \sum_{j,k=1}^{N_{\text{pod}}} Q_{ijk} y_j y_k \\ y_i(t_0) = \left(\hat{U}(\cdot, t_0) - \overline{\hat{U}}, \Phi_i\right) \end{cases}$$

Reduced order model : quadratic polynomial ODE system

Von Kármán instability $M = 0.85$: POD basis extraction

Database : 100 successive snapshots ($N_t = 100$) over one von Kármán period via Navier-Stokes simulation ($R_e = 5000$ and $M = 0.85$)

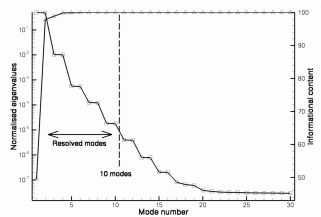

10 POD modes are considered

$$I_{N_{pod}} = \frac{\sum_{i=1}^{N_{pod}} \lambda_i}{\sum_{i=1}^{N_t} \lambda_i} \times 100 \approx 99.9\% \text{ if } N_{pod} = 10$$

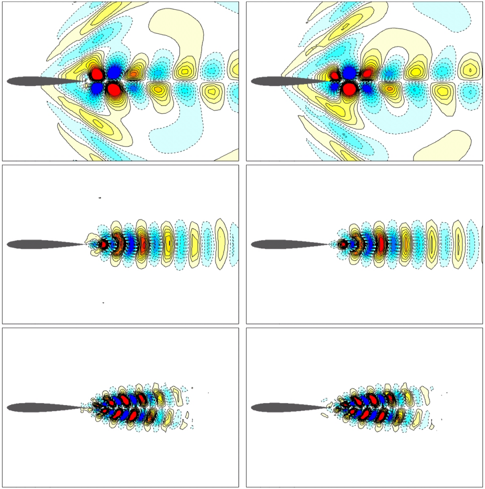

First six modes $\Phi_i^p(x)$

Von Kármán instability $M = 0.85$: temporal POD modes

First six modes $y_i(t)$

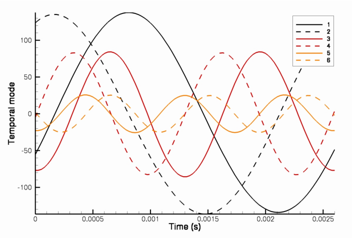

Reference temporal dynamics

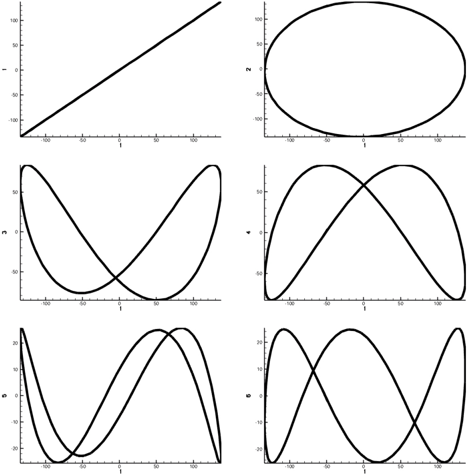

Von Kármán instability $M = 0.85$: low-order model

First six modes $y_i(t)$: prediction by ROM

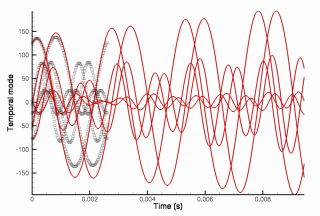

Reference temporal dynamics (black) and prediction by POD-Galerkin ROM (red)

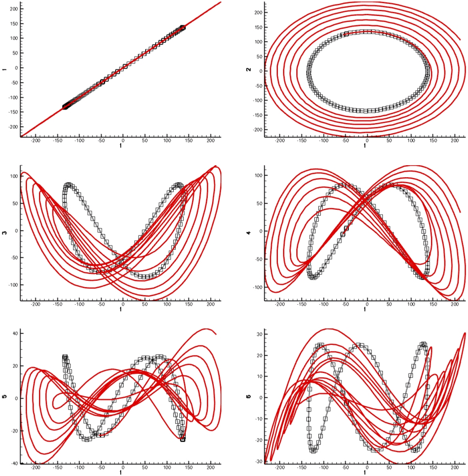

Amplitude growth and phase-lag : inherent instability

Noack *et al.* JFM2003

but relevant predictions for short-time integrations

Time integration : fourth-order-accurate Runge-Kutta scheme

Inherent instability of POD

What ?

The POD model is a dynamic model.
It has been observed that most mode coefficients are subject to module increasing.
Simplified examples (Noack *al.* JFM 2005) show the instability is inherent to model.
Consequence is accuracy only on a very short time.

What cure ?

Add viscosity (Podvin *et al.* JFM 1998)
Change scalar product (H^1, Iollo *et al.*TCFD 2000)
Add dissipation, to be calibrated.

Stabilisation strategy - calibration procedure

Calibrated dissipation in ROM :

$$\dot{y}_i^{\mathrm{rom}} = (C_i + C_i^s) + \sum_{j=1}^{N_{\mathrm{pod}}} (L_{ij} + L_{ij}^s)\, y_j^{\mathrm{rom}} + \sum_{j,k=1}^{N_{\mathrm{pod}}} Q_{ijk} y_j y_k = f_i\left(C^s, L^s, y^{\mathrm{rom}}\right)$$

Least square approach (Couplet-Basdevant-Sagaut JCP2005)

- Prediction error with respect to reference dynamic derivatives :

$$J\left(C^s, L^s\right) = \frac{1}{2} \sum_{i=1}^{N_{\mathrm{pod}}} \sum_{j=1}^{N_t} \left(\dot{y}_i(t_j) - f_i\left(C^s, L^s, y^{\mathrm{rom}}(t_j)\right)\right)^2$$

  where y^{rom} are predicted dynamics, “Poincaré calibration”

- Prediction error with respect to reference dynamics : “Floquet calibration”

$$J\left(C^s, L^s\right) = \frac{1}{2} \sum_{i=1}^{N_{\mathrm{pod}}} \sum_{j=1}^{N_t} \left(y_i(t_j) - y_i(t_0) - \int_{t_0}^{t_j} f_i\left(C^s, L^s, y^{\mathrm{rom}}(t)\right) dt\right)^2$$

- In practice : y^{rom} replaced by reference dynamics $\Rightarrow$ linear system

Back to *von Kármán* instability : calibrated ROM

First six modes $y_i(t)$: prediction by ROM

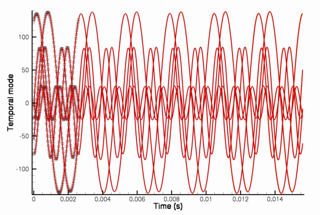

Reference temporal dynamics (black) and prediction by POD-Galerkin calibrated ROM by means of J minimisation (red, here Poincaré calibration)

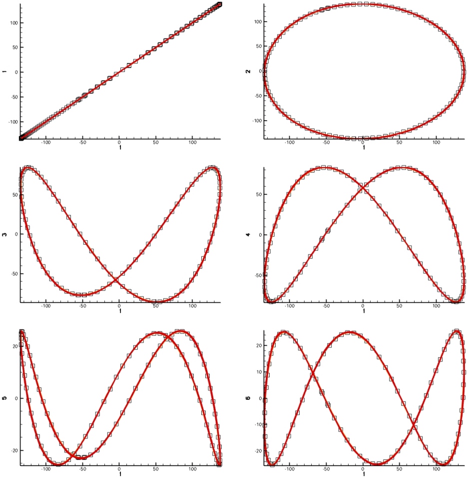

Stability
No phase-lag

Von Kármán instability $M = 0.85$: state variable prediction

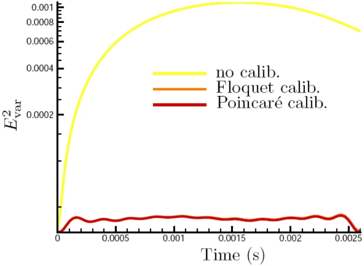

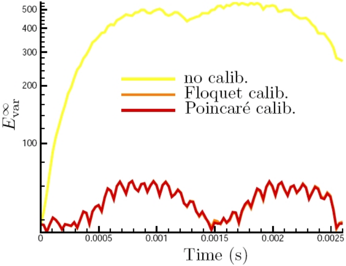

$$E^2_{\text{var}}(t) = \frac{\|v - v^{\text{rom}}\|_\Omega}{\|v\|_\Omega} \text{ , } E^\infty_{\text{var}}(t) = \max_i \max_{\mathbf{x}\in\Omega} |v_i - v_i^{\text{rom}}|$$

Similar results reached by both stabilised ROMs

$\rightarrow$ faithful prediction of state variable unsteadiness

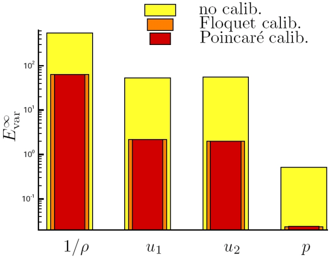

Von Kármán instability $M = 0.85$: R_e number variation

From $R_e = 5000$ to $R_e = 10000$: unique composite POD basis

$$Z_{mix} = \left\{ (v_{5000})_1 - \overline{v_{5000}}, \dots, (v_{5000})_{N_t} - \overline{v_{5000}}, (v_{10000})_1 - \overline{v_{10000}}, \dots, (v_{10000})_{N_t} - \overline{v_{10000}} \right\}$$

$y_i(t) =$
$(\hat{U}(.,t) - \overline{\hat{U}}, \Phi_i)$
$\zeta_i =$
$\frac{1}{T_s} \int_{t_0}^{t_0+T_s} y_i^2 \, dt$

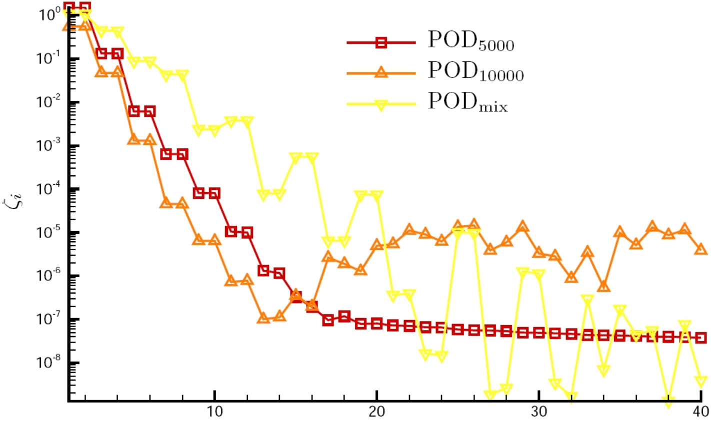

Informational content conveyed by three different POD basis at $R_e = 5000$ and $M_a = 0.85$

Von Kármán instability $M = 0.85$: R_e number variation

Three strategies are compared for modifying R_e number in the ROM

Reynolds number can be changed by changing viscosity or inflow velocity.

- From ROM_{10000}, varying viscosity, same mean flow
- Interpolation (linear or quadratic) of mean flows, control function (forcing) $\rightarrow$ state variable prediction
- Interpolation of all ODE coefficients

Comparisons :

- Three ROMs based on two Navier-Stokes simulations
- Three ROMs based on three Navier-Stokes simulations
- Intermediate reference Navier-Stokes simulations

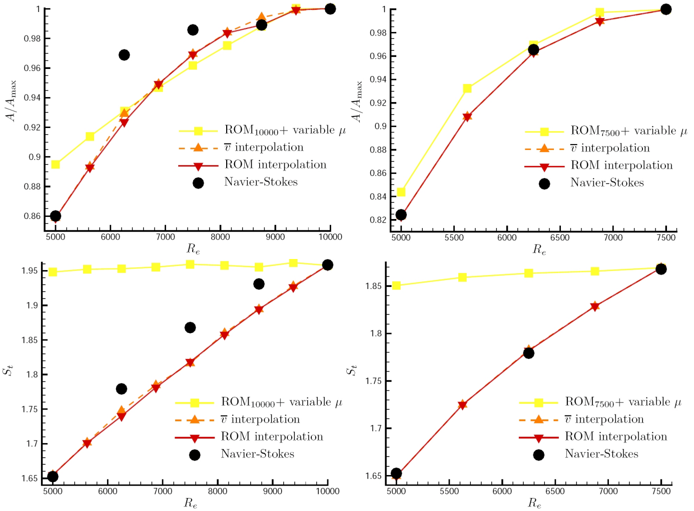

- Varying μ allows an efficient capture of amplitude variation but not Strouhal number evolution
- Interpolation approaches (even linear) lead to faithfull non-linear behaviours, and exact predictions of resolved configurations
- Refinement of course improves ROM predictive capacities

Variation of the normalised maximum amplitude and Strouhal number of the first POD dynamic as a function of R_e number for $5000 \le R_e \le 10000$ (left) and $5000 \le R_e \le 7500$ (right)

POD analysis of buffet phenomenon

Flow past a NACA0012 airfoil at zero angle of incidence, $R_e = 10000$ and $M = 0.80$: interaction between von Kármán mode I and mode II (buffet)

First six modes $\Phi_i^p(x)$

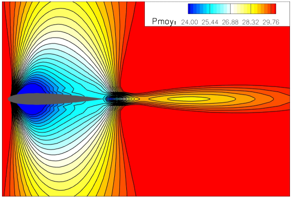

Averaged pressure

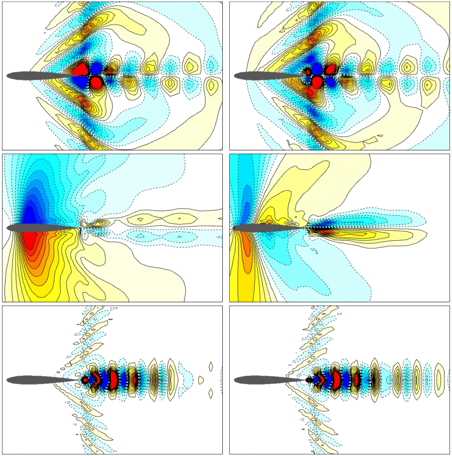

3rd and 4th POD modes : "buffet modes"

Buffet configuration $M = 0.80$: temporal modes

First eight modes $y_i(t)$

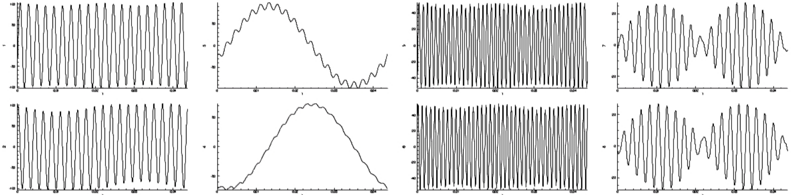

2200 snapshots over one buffet period ($\approx$ 20 von Kármán periods)

$$N_{pod} = \color{red}{16}$$

$$\rightarrow I_{N_{pod}} \approx 99.9\%$$

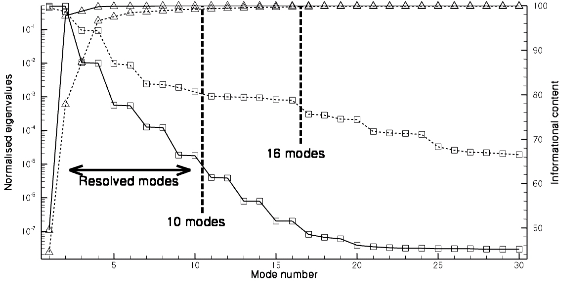

First eight predicted modes $y_i(t)$

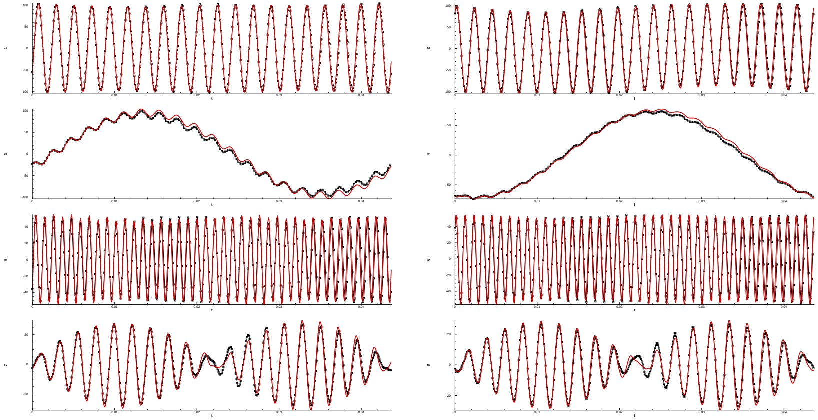

Prediction of the state variables
Pressure

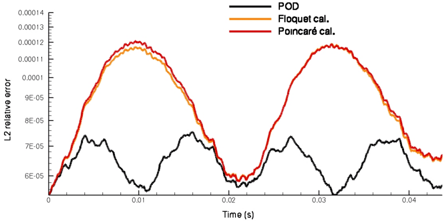

Reconstruction errors over one buffet period : POD filtering (black) and calibated ROMs prediction error (orange and red)

$$E^2_{\mathrm{var}}(t) = \frac{\|v - v^{\mathrm{rom}}\|_\Omega}{\|v\|_\Omega}$$

Reliable prediction over snapshot temporal horizon

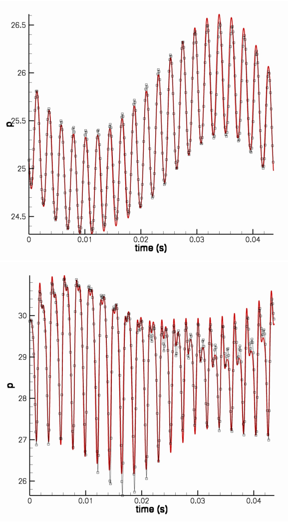

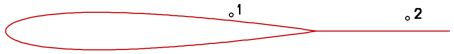

Buffet configuration $M = 0.80$: state variable prediction

Velocity and pressure fields after one buffet period (- - : ROM)

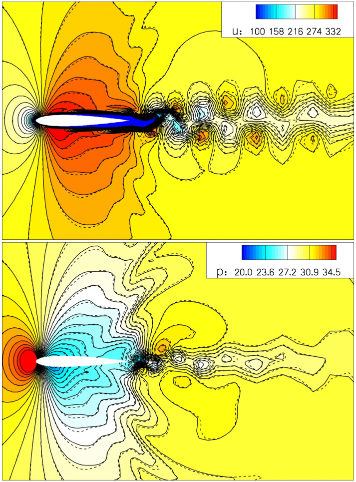

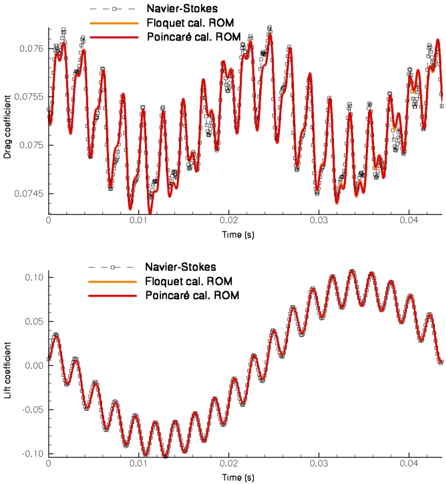

Prediction of the unsteady aerodynamic coefficients over NS temporal horizon

Conclusions

- **Compressible POD-Galerkin model** relying on quadratic-flux variables and involving coherent scalar product.
- The model enables a *faithfull prediction* of the complex instability mode interaction in the high-transonic regime while *numerical complexity is highly reduced*
- Calibrated ROM : stability, respect of the phase $\rightarrow$ useful tool for stability analysis
- Physical investigation of **high-transonic regime physics** : von Kármán and buffet modes, on the basis of Navier-Stokes simulation and low-order modelling
- ROM robustness to prediction of intermediate Reynolds.